11734 *Inorg. Chem.* **2009**, *48*, 11734–11742
DOI: 10.1021/ic901789h

Inorganic Chemistry
Article

Redox Processes in the Iron(III)/9,10-Phenanthraquinone System

Petr Milko[†] and Jana Roithová*[,†,‡]

[†]*Institute of Organic Chemistry and Biochemistry, Academy of Sciences of the Czech Republic, Flemingovo nám. 2, 16610 Praha 6, Czech Republic and* [‡]*Department of Organic Chemistry, Faculty of Sciences, Charles University in Prague, Hlavova 8, 12843 Prague 2, Czech Republic*

Received September 7, 2009

With the use of the model complexes $[(PQ)FeCl(CH_3O)]^+$, $[(phen)FeCl(CH_3O)]^+$, and $[(PQ)(phen)FeCl(CH_3O)]^+$, where PQ is 9,10-phenanthraquinone and phen is 1,10-phenanthroline, the reactivity of phenanthraquinone in complexes with iron(III) is investigated. It is shown that 9,10-phenanthraquinone takes part in redox processes occurring at iron and thereby allows the oxidation of methanolate to formaldehyde. The oxidation is driven by the reduction of iron(III) to iron(II) and 9,10-phenanthraquinone to the semihydroquinone radical or semiquinolate, if the hydrogen atom is transferred from methanolate to chlorine rather than PQ. 1,10-Phenanthroline, on the other hand, acts as an innocent ligand, and the $[(phen)FeCl(CH_3O)]^+$ complex shows a typical two-state reactivity. The reactivity of $[(PQ)(phen)FeCl(CH_3O)]^+$ reveals that the hexacoordination of iron energetically facilitates the oxidation of methanolate, and therefore it is proposed that, in the presence of suitable reductants, the mixture of iron(III) and 9,10-phenanthraquinone can lead to the generation of the semihydroquinone radicals, species responsible for the toxicity of PQ. The fragmentation of $[(PQ)(phen)FeCl(CH_3O)]^+$ also demonstrates a strong binding of phen toward iron(III), which is a reason for using phen as an iron chelator in biochemistry. The structures and reactivities of the complexes are investigated by means of mass spectrometry, infrared multiphoton dissociation spectra, and density functional theory calculations.

Introduction

Diesel exhaust particles (DEPs) play a negative role in inducing pathogenic processes such as lung cancer, allergies, or asthma.[1−3] The toxic principle of DEPs is ascribed to absorbed organic compounds (aliphatic hydrocarbons, polycyclic aromatic hydrocarbons, heterocyclic compounds, and various oxidized derivatives). It has been shown that the exposure of cell cultures to the organic extract from DEPs leads to the generation of reactive oxygen species and consequently to oxidative stress.[4] For example, quinones undergo enzymatic and nonenzymatic redox cycling with their corresponding semiquinone radicals, which can transfer electrons to oxygen molecules and thereby generate superoxide anion radicals $O_2^{-\bullet}$.[5] Reactions of $O_2^{-\bullet}$ lead to hydrogen peroxide, which further decompose by the Haber-Weiss reaction[6,7] to the hydroxide anion and hydroxy radical, the latter being responsible for the oxidative degradation of essential macromolecules.

One of the major quinones occurring in DEPs is 9,10-phenanthraquinone (PQ). The corresponding semiquinolate $PQ^{-\bullet}$ can be produced by the reduction of PQ with enzymes such us NADPH-cytochrome P450 reductase[8,9] or neuronal nitric oxide synthase[10] or in reactions with thiol-containing proteins.[11,12] Phenanthrasemiquinolate then transfers an electron to an oxygen molecule, and the intracellular iron (or other metal ions) catalyzes the subsequent reaction toward the production of hydroxy radicals.[13] It has been shown that the addition of iron chelators, such as 1,10-phenanthroline (phen), blocks the production of

*To whom correspondence should be addressed. E-mail: roithova@natur.cuni.cz.

(1) Schuetzle, D.; Lee, F. S.; Prater, T. J. *Int. J. Environ. Anal. Chem.* **1981**, *9*, 93.
(2) McClellan, R. O. *Annu. Rev. Pharmacol. Toxicol.* **1987**, *27*, 279.
(3) Nel, A. E.; Diaz-Sanchez, D.; Li, N. *Curr. Opin. Pulm. Med.* **2001**, *7*, 20.
(4) Sagai, M.; Saito, H.; Ichinose, T.; Kodama, M.; Mori, Y. *Free. Radical Biol. Med.* **1993**, *14*, 37.
(5) Bolton, J. L.; Trush, M. A.; Penning, T. M.; Dryhurst, G.; Monks, T. J. *Chem. Res. Toxicol.* **2000**, *13*, 135.
(6) Harber, F.; Weiss, J. *Proc. R. Soc. London* **1934**, *147*, 332.
(7) Halliwell, B.; Gutteridge, J. M. C. *Free Radicals in Biology and Medicine*, 3rd ed.; Oxford University Press: Oxford, U. K., 1999.
(8) Kumagai, Y.; Arimoto, T.; Shinyashiki, M.; Shimojo, N.; Nakai, Y.; Yoshikawa, T.; Sagai, M. *Free Radical Biol. Med.* **1997**, *22*, 479.
(9) Sugimoto, R.; Kumagi, Y.; Nakai, Y.; Ishii, T. *Free Radical Biol. Med.* **2005**, *38*, 388.
(10) Kumagai, Y.; Nakajima, H.; Midorikawa, K.; Homma-Takeda, S.; Shimojo, N. *Chem. Res. Toxicol.* **1998**, *11*, 608.
(11) Kumagai, Y.; Koide, S.; Taguchi, K.; Endo, A.; Nakai, Y.; Yoshikawa, T.; Shimojo, N. *Chem. Res. Toxicol.* **2002**, *15*, 483.
(12) Liebeke, M.; Pother, D. C.; van Duy, N.; Albrecht, D.; Becher, D.; Hochgrafe, F.; Lalk, M.; Hecker, M.; Antelmann, H. *Mol. Microbiol.* **2008**, *69*, 1513.
(13) Jarabak, R.; Harvey, R. G.; Jarabak, J. *Chem.-Biol. Int.* **1998**, *115*, 201.

 Published on Web 11/23/2009

Scheme 1. Sketch of Various Redox Forms of 9,10-Phenanthraquinone with Labels Used Throughout the Paper

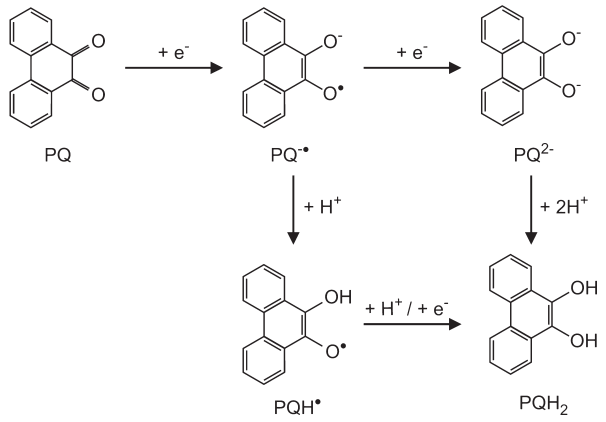

hydroxy radicals, which has been ascribed to the suppression of the transformation of hydrogen peroxide to the hydroxyl radical.[9,14] Here, we address the essential questions, how 9,10-phenanthraquinone (Scheme 1) interacts with iron(III) itself and how the iron(III)/phenanthraquinone complex behaves in the presence of electron and proton donors.[15−20]

Experimental Section

The experiments were performed with a TSQ Classic mass spectrometer with a QOQ configuration (Q stands for quadrupole and O stands for octopole), described in detail elsewhere.[21] The ions of interest were generated by electrospray ionization (ESI) from methanolic solutions of $FeCl_3$ and the ligands 9,10-phenanthraquinone and 1,10-phenanthroline. The first quadrupole is used to record source spectra or to mass-select the desired ions. The mass-selected ions are collided with xenon ($p_{Xe} \cong 0.08$ mTorr) in the octopole collision cell, and the fragments are analyzed by Q2. The collision energy is determined by the potential offset between Q1 and O, and the energy resolution is typically 1.2 ± 0.1 eV (full width at half-maximum). Variation of the collision energy leads to the breakdown diagrams that allow an approximate determination of appearance energies (AEs) of the various fragmentation channels.[22−25]

The gas-phase infrared (IR) spectra of the desired ions were recorded using a Bruker Esquire 3000 ion trap mounted on a free electron laser CLIO (Centre Laser Infrarouge Orsay, France), providing photons with wavenumbers roughly from 900 cm^{-1} to 1800 cm^{-1}.[26] The desired ions were generated by ESI, mass-selected, and stored in the ion trap. The laser beam was admitted to the ion trap in four macropulses. The dependence of the intensity of the ion fragmentation on the wavelength of the photons provides infrared multiphoton dissociation (IRMPD) spectra, because the dissociation is induced only if the parent ions absorb photons at a given wavelength.[27,28]

The calculations are performed using the density functional method B3LYP[29−32] in conjunction with the 6-311++G** basis sets, as implemented in the Gaussian 03 suite.[33] This approach has been shown as suitable for other iron systems and quinones.[16,34,35] For all optimized structures, frequency analyses at the same level of theory are used in order to assign them as genuine minima or transition structures on the potential-energy surface as well as to calculate harmonic vibration frequencies and zero-point vibrational energies. The relative energies (E_{rel}) of the structures given below refer to energies at 0 K. For a comparison of infrared spectra with the experimental results, the frequencies were scaled by 0.985. Complexes of iron and phenanthraquinone, $\mathbf{2}^+$−$\mathbf{5}^+$, $\mathbf{7}^+$, $\mathbf{TS1}^+/\mathbf{3}^+$, $\mathbf{19}^+$, and $\mathbf{20}^+$ bear radical sites at PQ as well as at iron, which leads to spin contaminations of the low spin-state (quartet) wave functions. We have applied corrections based on the broken-symmetry approach,[36−38] which however resulted in energy differences on the order of 10^{-2} eV (details of the method as well as the results can be found in the Supporting Information). With regard to the negligible effects, we use the uncorrected energies here.

Results and Discussion

The intrinsic aspects of the interaction between iron(III) and phenanthraquinone are studied in the isolated complexes in the gas phase. For a detailed study, we have chosen complex $[(PQ)FeCl(CH_3O)]^+$, which contains chloride and methanolate as the counterions. Methanolate can be oxidized to formaldehyde, which is associated with the transfer of two electrons and one proton to the remaining part of the complex. This complex therefore offers a unique variety of possible redox processes of potential biochemical interest. For the particular effect of the phenanthraquinone−iron interaction, we will also compare the results with the reactivity of an analogous complex containing 1,10-phenanthroline (phen), $[(phen)FeCl(CH_3O)]^+$.

Electrospray ionization of a methanolic solution of $FeCl_3$ and phenanthraquinone leads to the generation of complexes $[(PQ)FeXY]^+$, where X,Y = Cl or CH_3O. As pointed out above, we have chosen the mixed complex $[(PQ)FeCl(CH_3O)]^+$ for a detailed study due to the presence

(14) Britton, R. S.; Leicester, K. L.; Bacon, B. R. *Int. J. Hematol.* **2002**, *76*, 219.
(15) Spike, G. H.; Bill, E.; Weyhermüller, T.; Wieghardt, K. *Angew. Chem., Int. Ed.* **2008**, *47*, 2973.
(16) Simaan, A. J.; Boillot, M.-L.; Carrasco, R.; Cano, J.; Girerd, J.-J.; Mattioli, T. A.; Ensling, J.; Spiering, H.; Gütlich, P. *Chem.—Eur. J.* **2005**, *11*, 1779.
(17) Shaikh, N.; Goswami, S.; Panja, A.; Wang, X.-Y.; Gao, S.; Butcher, R. J.; Banerjee, P. *Inorg. Chem.* **2004**, *43*, 5908.
(18) Pierpont, C. G.; Lange, C. W. *Prog. Inorg. Chem.* **1994**, *41*, 331.
(19) Pierpont, C. G. *Coord. Chem. Rev.* **2001**, *219*, 415.
(20) Roithová, J.; Schröder, D. *Coord. Chem. Rev.* **2009**, *253*, 666.
(21) (a) Roithová, J.; Schröder, D. *Phys. Chem. Chem. Phys.* **2007**, *9*, 731. (b) Roithová, J.; Schröder, D.; Míšek, J.; Stará, I. G.; Starý, I. *J. Mass Spectrom.* **2007**, *42*, 1233.
(22) Schröder, D.; Engeser, M.; Brönstrup, M.; Daniel, C.; Spandl, J.; Hartl, H. *Int. J. Mass Spectrom.* **2003**, *228*, 743.
(23) Most of the fragmentations observed do not correspond to direct bond cleavages but are associated with at least one rearrangement. We therefore refrain from using sophisticated evaluations of the appearance energies[24,25] and only qualitatively compare various channels.
(24) Narancic, S.; Bach, A.; Chen, P. *J. Phys. Chem. A* **2007**, *111*, 7006.
(25) Armentrout, P. B.; Ervin, K. M.; Rodgers, M. T. *J. Chem. Phys.* **2008**, *112*, 10071.
(26) Mac Aleese, L.; Simon, A.; McMahon, T. B.; Ortega, J. M.; Scuderi, D.; Lemaire, J.; Maitre, P. *Int. J. Mass Spectrom.* **2006**, *249*, 14.
(27) Dopfer, O. *J. Phys. Org. Chem.* **2006**, *19*, 540.
(28) Polfer, N. C.; Oomens, J. *Phys. Chem. Chem. Phys.* **2007**, *9*, 3804.
(29) Vosko, S. H.; Wilk, L.; Nusair, M. *Can. J. Phys.* **1980**, *58*, 1200.
(30) Lee, C.; Yang, W.; Parr, R. G. *Phys. Rev. B* **1988**, *37*, 785.
(31) Becke, A. D. *Phys. Rev. A* **1988**, *38*, 3098.
(32) Miehlich, B.; Savin, A.; Stoll, H.; Preuss, H. *Chem. Phys. Lett.* **1989**, *157*, 200.
(33) *Gaussian 03*, revision E.01; Frisch, M. J., Ed.; et al. Gaussian, Inc.: Wallingford, CT, 2004.
(34) Borowski, T.; Bassan, A.; Siegbahn, P. E. M. *Inorg. Chem.* **2004**, *43*, 3277.
(35) Wheeler, D. E.; Rodriguez, J. H.; McCusker, J. K. *J. Phys. Chem. A* **1999**, *103*, 4101.
(36) Schlegel, H. B. *J. Chem. Phys.* **1986**, *84*, 4530.
(37) Noodleman, L. *J. Chem. Phys.* **1981**, *74*, 5737.
(38) Yamaguchi, K.; Jensen, F.; Dorigo, A.; Houk, K. N. *Chem. Phys. Lett.* **1988**, *149*, 537.

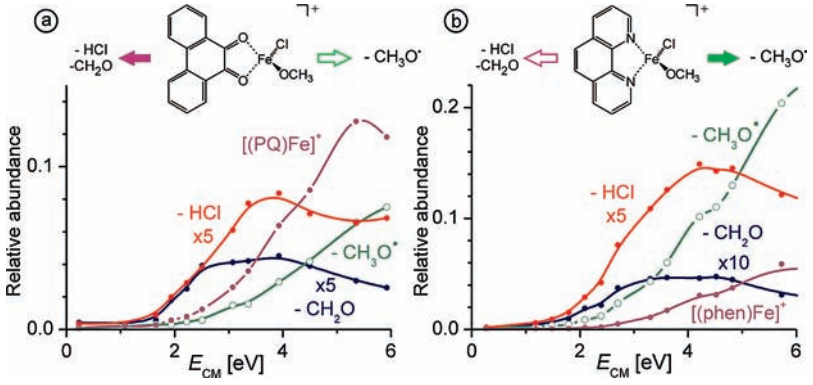

Figure 1. Relative abundances of the fragmentations of $[(PQ)FeCl(CH_3O)]^+$ (a) and $[(phen)FeCl(CH_3O)]^+$ (b) dependent on the collision energy (the losses of $CH_3O^•$ are in green, CH_2O in blue, HCl in red, and the combined losses of CH_2O and HCl in violet). Note that the losses of HCl and CH_2O are enhanced by a given factor.

of a potential proton and electron donor CH_3O^-.[39] The collision-induced dissociation (CID) of the mass-selected complex $[(PQ)FeCl(CH_3O)]^+$ shows a competition of two major processes. On the one hand, the closed-shell molecules of formaldehyde and HCl are eliminated, which is necessarily associated with some rearrangements within the complex. These fragmentations appear at low collision energies (Figure 1a). On the other hand, the methanolate counterion is eliminated as a radical, which is kinetically preferred, and its abundance increases with increasing collision energy. The formation of the naked $[(PQ)Fe]^+$ complex appears at lower collision energies than the methoxy loss, and therefore, at least at low collision energies, it originates from the subsequent eliminations of two closed-shell molecules CH_2O and HCl, rather than two radicals $CH_3O^•$ and $Cl^•$.

The preferential elimination of HCl and CH_2O implies that either the structure of the investigated complex is different than suggested or facile rearrangements of hydrogen atoms among the ligands are occurring. We have performed a DFT study in order to shed light on the role of the 9,10-phenanthraquinone ligand in the redox processes within the model system $[(PQ)FeCl(CH_3O)]^+$ ($\mathbf{1}^+$).[40] The ground state of the complex $[(PQ)FeCl(CH_3O)]^+$ is a sextet ($^6\mathbf{1}^+$, Figure 2). The quartet ($^4\mathbf{1}^+$) and the doublet ($^2\mathbf{1}^+$) states lie 0.77 and 1.57 eV, respectively, higher in energy.[41−44] The PQ ligand is fully oxidized in all states localized for this structure (Scheme 3).

The alternative isomer $[(PQ)Fe(HCl)(CH_2O)]^+$ ($\mathbf{2}^+$) bears neutral HCl and CH_2O as ligands and could therefore readily explain the facile losses of these molecules. The calculations show that the sextet state of this isomer ($^6\mathbf{2}^+$) lies 0.81 eV higher in energy than $^6\mathbf{1}^+$. The energy barrier associated with the hydrogen rearrangement between the two ligands (^{6}TS$\mathbf{1}^+/\mathbf{2}^+$) amounts to 1.74 eV. Analysis of the wave function reveals that the oxidation of methanolate to formaldehyde proceeds at the expense of iron(III) being reduced to iron(II) and phenanthraquinone being reduced to phenanthrasemiquinolate ($PQ^{-•}$). The unpaired electron localized at phenanthrasemiquinolate can undergo a spin-flip, leading to the low-spin quartet state $^4\mathbf{2}^+$ lying 0.08 eV below the corresponding sextet state (Scheme 2). Note however that the spin flip at the $PQ^{-•}$ ligand might be hindered by a small spin−orbit coupling and can be thus slow.[45] In any case, the reactivity observed here can be fully explained involving only the sextet state.

Further, an excited quartet state is obtained from $^6\mathbf{2}^+$ by a spin-flip at the iron center (0.44 eV above $^6\mathbf{2}^+$). The quartet transition state (^{4}TS$\mathbf{1}^+/\mathbf{2}^+$)* lies lower in energy than ^{6}TS$\mathbf{1}^+/\mathbf{2}^+$, and spin-coupling might therefore effectively lower the barrier for the hydrogen migration among the ligands. For an easier orientation, the electron configurations of the parent ion $\mathbf{1}^+$ and the two-electron reduction product $\mathbf{2}^+$ are shown in Scheme 2.

The formaldehyde molecule can also be formed by a hydrogen migration to the phenanthraquinone ligand. The energy barrier for this process (^{6}TS$\mathbf{1}^+/\mathbf{3}^+$) amounts to 1.90 eV and thus is slightly higher than ^{6}TS$\mathbf{1}^+/\mathbf{2}^+$. The isomer $[(PQH)FeCl(CH_2O)]^+$ ($^6\mathbf{3}^+$) is almost isoenergetic with $^6\mathbf{1}^+$ ($E_{rel}(^6\mathbf{3}^+) = 0.05$ eV) and contains iron(II) and the phenanthrasemihydroquinone radical. The spin-flip at the phenanthrasemihydroquinone radical leads to the quartet state $^4\mathbf{3}^+$, which lies 0.06 eV lower in energy than $^6\mathbf{3}^+$.

The identity of the investigated complex generated by ESI can be unraveled by a comparison of the experimental IRMPD spectrum of the complex with the theoretical infrared spectra calculated for the possible isomers (Figure 2b−d). The experimental spectrum contains three major peaks at 1574, 1454, and 1312 cm^{-1}. All peaks are nicely reproduced by the theoretical spectrum of the $[(PQ)FeCl(CH_3O)]^+$ isomer ($^6\mathbf{1}^+$, Figure 2c) with the calculated CO vibration at 1580 cm^{-1} and the C−C stretching modes of PQ at 1461 and 1327 cm^{-1}, respectively. On the other hand, the IR spectra of isomers $^6\mathbf{2}^+$ and $^6\mathbf{3}^+$ (Figure 2b and d, respectively) completely disagree with the experiment, and therefore the presence of these isomeric ions among the generated ions is excluded. We note in passing that the IR spectra of the complexes in the quartet states are almost identical with those in sextet states, and therefore assigning of the electronic state is less definite. However, the spectrum of $^6\mathbf{1}^+$ fits the experimental data

(39) We did not investigate the complex with two methanolates, because of the more demanding computations associated with the problem.
(40) Trage, C.; Diefenbach, M.; Schröder, D.; Schwarz, H. *Chem.—Eur. J.* **2006**, *12*, 2454.
(41) Clemmer, D. E.; Chen, Y.-M.; Khan, F. A.; Armentrout, P. B. *J. Phys. Chem.* **1994**, *98*, 6522.
(42) Fiedler, A.; Hrušák, J.; Koch, W.; Schwarz, H. *Chem. Phys. Lett.* **1993**, *211*, 242.
(43) Irigoras, A.; Fowler, J. E.; Ugalde, J. M. *J. Am. Chem. Soc.* **1999**, *121*, 8549.
(44) Yoshizawa, K. *Acc. Chem. Res.* **2006**, *39*, 375.
(45) (a) Poli, R.; Harvey, J. N. *Chem. Soc. Rev.* **2003**, *32*, 1. (b) Harvey, J. N. *Phys. Chem. Chem. Phys.* **2007**, *9*, 331.

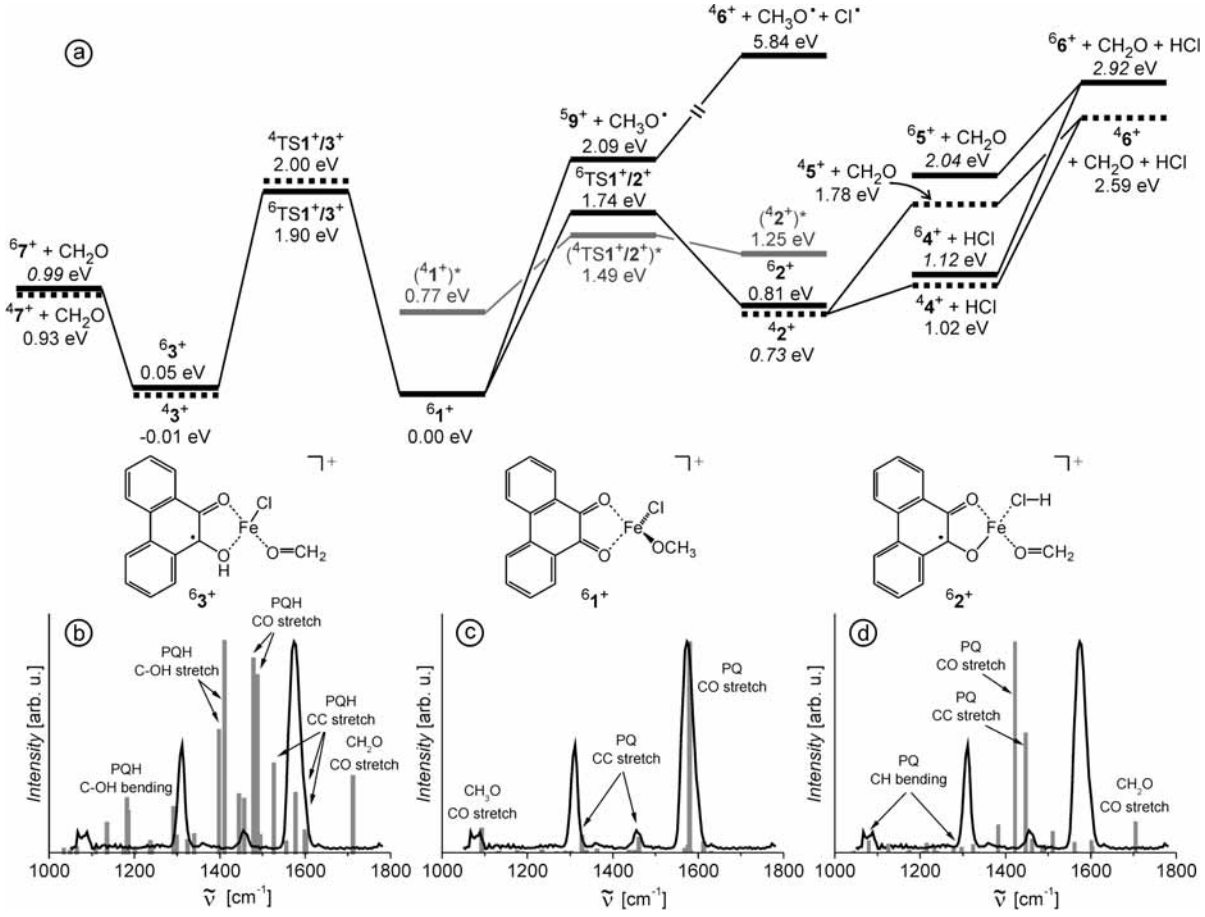

Figure 2. (a) Potential-energy surface of $[(PQ)FeCl(CH_3O)]^+$ ($\mathbf{1}^+$) associated with its rearrangements and fragmentations. The black solid lines correspond to the sextet state, and the black dashed lines represent the quartet states associated with the sextet states by a spin-flip at the PQ ligand. The gray lines correspond to the excited quartet state (low-spin at iron). Energies are given at 0 K relative to $E^{0K}(^6\mathbf{1}^+) = -2527.694725$ hartree; energies in italics correspond to single-point calculations at geometries optimized for the corresponding low- or high-spin state. The experimental IRMPD spectrum of the $[(PQ)FeCl(CH_3O)]^+$ complex (black line) is compared with the theoretical spectra (scaled by 0.985) of $^6\mathbf{3}^+$ (b), $^6\mathbf{1}^+$(c), and $^6\mathbf{2}^+$ (d) (bar spectra).

Scheme 2

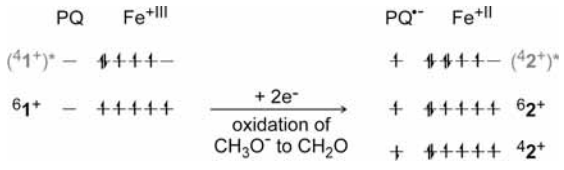

slightly better than those of $^4\mathbf{1}^+$ and $^2\mathbf{1}^+$ (see Figure S5 in the Supporting Information).

We have shown previously that the C−O stretching vibration is a sensitive spectral marker of the oxidation state of the phenoxy ligands.[46] Specifically, the wavenumbers around 1300 cm^{-1} indicate the reduced phenolate form, whereas the values around 1500 cm^{-1} point toward the phenoxy radical form of the ligand. Here, the C−O vibrations located around 1580 cm^{-1} show that the phenanthraquinone ligand is in the oxidized form with CO double bonds. Markedly, the C−O vibrations for the alternative structure $[(PQ)Fe(HCl)(CH_2O)]^+$ ($\mathbf{2}^+$) are red-shifted by more than 150 cm^{-1} (Scheme 3), which demonstrates the above-mentioned partial reduction of the PQ ligand to the phenanthrasemiquinolate form PQ$^{-•}$. Similarly, the formation of phenanthrasemihydroquinone in $\mathbf{3}^+$ is associated with a red shift of the C−OH stretching mode roughly by 170 cm^{-1}, and the CO mode is roughly 100 cm^{-1} red-shifted. Further, the red shift of CO vibrations nicely correlates with the prolongation of both CO bonds.

The calculated potential-energy surface in Figure 2a provides a rationale for all observed fragmentation channels. The fragmentation of $[(PQ)Fe(HCl)(CH_2O)]^+$ ($\mathbf{2}^+$) leads either to $[(PQ)Fe(CH_2O)]^+$ ($\mathbf{4}^+$) + HCl ($E_{rel}(^4\mathbf{4}^+ + HCl)$ = 1.02 eV and $E_{rel}(^6\mathbf{4}^+ + HCl)$ = 1.12 eV[47]) or to $[(PQ)Fe(HCl)]^+$ ($\mathbf{5}^+$) + CH_2O ($E_{rel}(^4\mathbf{5}^+ + CH_2O)$ = 1.78 eV and $E_{rel}(^6\mathbf{5}^+ + CH_2O)$ = 2.04 eV[47]). The consecutive elimination of both neutral molecules from $\mathbf{2}^+$ leads to bare $[(PQ)Fe]^+$ ($\mathbf{6}^+$) and requires $E_{rel}(^4\mathbf{6}^+ + CH_2O + HCl)$ = 2.59 eV ($E_{rel}(^6\mathbf{6}^+ + CH_2O + HCl)$ = 2.92 eV[47]). Optimized geometries of all fragments can be found in Scheme 4.

Obviously, the fragmention pathway leading via the intermediate $\mathbf{2}^+$ energetically favors the elimination of HCl over CH_2O, and therefore the HCl loss prevails in the experiment. However, the comparable abundances of the HCl and CH_2O eliminations at low collision energies (up to 2.5 eV) point toward an alternative mechanism for the CH_2O elimination. Such a channel might be represented by the rearrangement of

(46) Milko, P.; Roithová, J.; Tsierkezos, N.; Schröder, D. *J. Am. Chem. Soc.* **2008**, *130*, 7186.

(47) The value was obtained by a single-point calculation at the geometry optimized for the corresponding quartet state.

Scheme 3. Optimized Structures of $[(PQ)FeCl(CH_3O)]^+$ and Its Isomers[a]

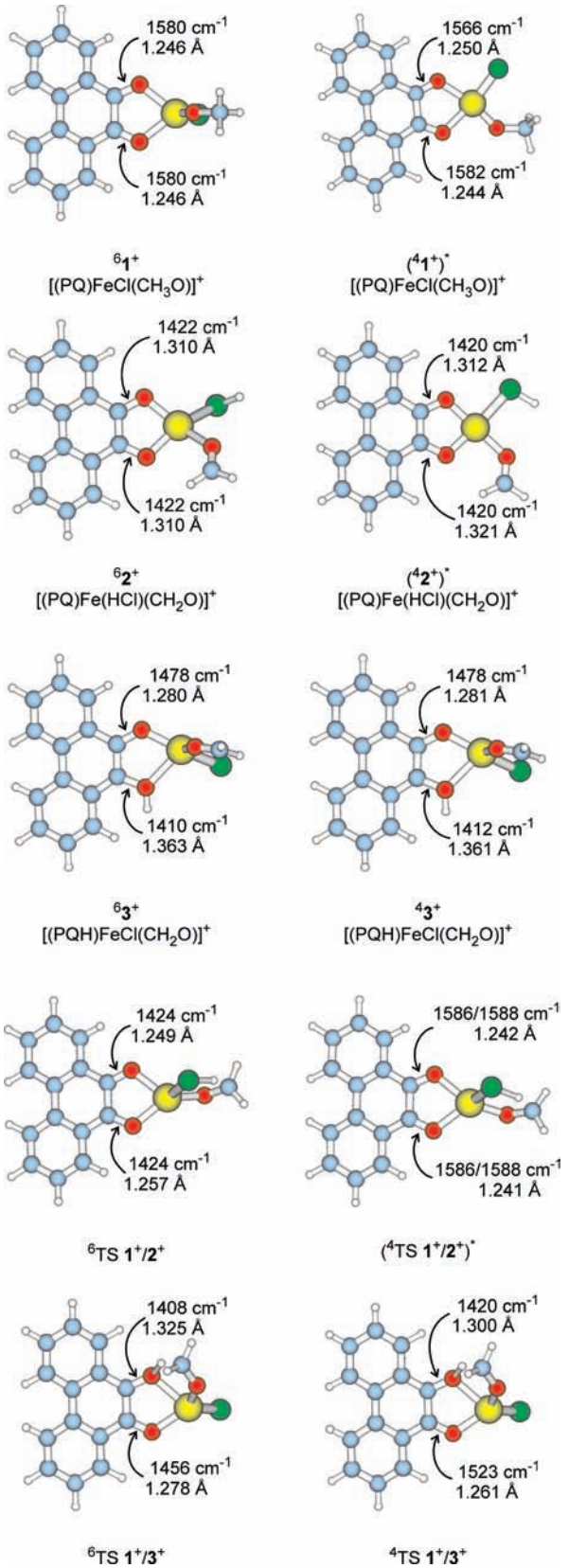

[a] The carbon atoms are in blue, oxygens in red, chlorines in green, hydrogens in white, and iron is yellow. The selected bond lengths are in ångstroms, and the wavenumbers correspond to the symmetric stretching vibrations of the corresponding CO bonds in cm^{-1}. More information can be found in the Supporting Information.

Scheme 4. Optimized Structures of the Elimination Products[a]

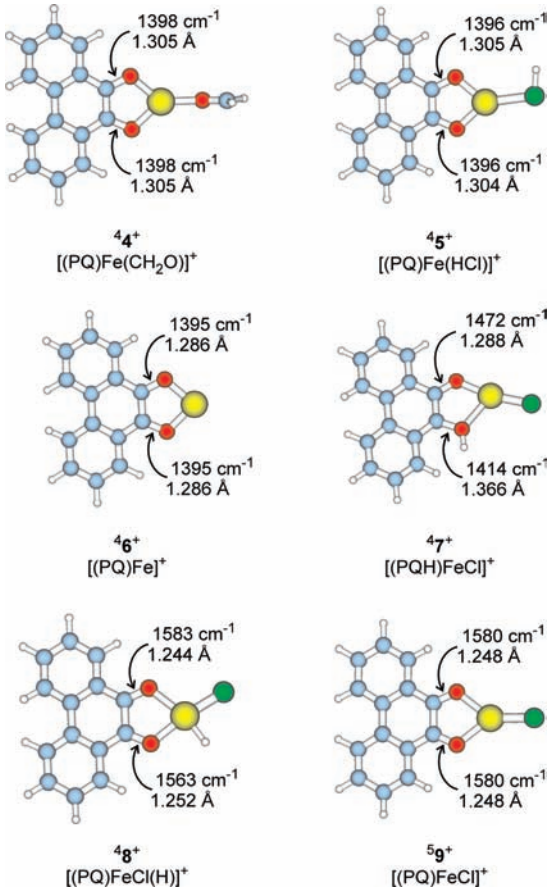

[a] The carbon atoms are in blue, oxygens in red, chlorines in green, hydrogens in white, and iron is yellow. The selected bond lengths are in ångstroms, and the wavenumbers correspond to the stretching vibrations of the corresponding CO bonds. More information can be found in the Supporting Information.

the starting complexes $\mathbf{1}^+$ to $\mathbf{3}^+$, which leads only to the elimination of formaldehyde ($E_{rel}({}^4\mathbf{7}^+ + CH_2O) = 0.93$ eV and $E_{rel}({}^6\mathbf{7}^+ + CH_2O) = 0.99$ eV[47]). We have also investigated a possible hydrogen migration from the methanolato ligand to the iron atom, which finally leads to the products $[(PQ)FeCl(H)]^+$ ($\mathbf{8}^+$) and CH_2O ($E_{rel}({}^4\mathbf{8}^+ + CH_2O) = 2.13$ eV[47,48]). This pathways, however, lies much higher in energy and is not considered further.

The eliminations of closed-shell molecules are thus determined by the competition between hydrogen transfers from the methanolato ligand of $[(PQ)FeCl(CH_3O)]^+$ ($\mathbf{1}^+$) either to chlorine or to phenanthraquinone, which finally determines the ratio of the HCl and CH_2O eliminations. The energy required for the combined loss of HCl and CH_2O is only slightly higher than the rearrangement barriers, and therefore this process prevails at larger collision energies. Finally, the direct expulsion of the methoxy radical from the parent complex requires 2.09 eV. This amount of energy is larger than both barriers for the rearrangements to $\mathbf{2}^+$ and $\mathbf{3}^+$ and the subsequent energy demands for the first elimination of a closed-shell molecule; therefore, closed-shell losses prevail over the methoxy loss. Surprisingly, the subsequent

(48) Iron is in the oxidation state Fe^{III} (quartet state), and phenanthraquinone is fully oxidized. The excited sextet state lies 1.26 eV higher in energy (single-point calculation).

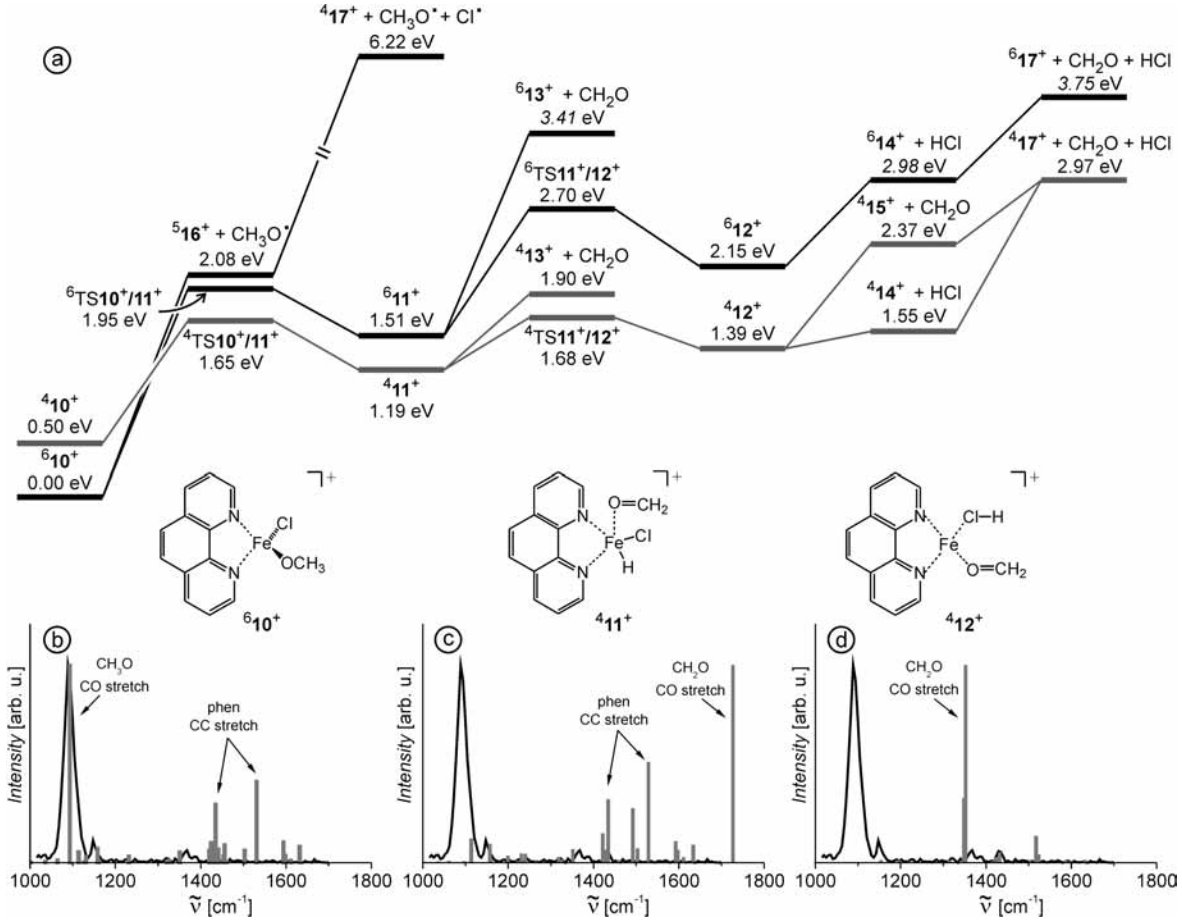

Figure 3. (a) Potential-energy surface of $[(phen)FeCl(CH_3O)]^+$ ($\mathbf{1}^+$) associated with its rearrangements and fragmentations. The black solid lines correspond to the sextet state, and the gray lines correspond to the quartet state (low-spin at iron). Energies are given at 0 K relative to $E^{0K}(^6\mathbf{10}^+) = -2410.546539$ hartree; energies in italics correspond to the single-point calculations at geometries optimized for the corresponding low- or high-spin state. The experimental IRMPD spectrum of the $[(phen)FeCl(CH_3O)]^+$ complex (black line) is compared with the theoretical spectra (scaled by 0.985) of $^6\mathbf{10}^+$ (b), $^4\mathbf{11}^+$(c), and $^4\mathbf{12}^+$ (d) (bar spectra).

eliminations of closed-shell molecules dominate even at larger collision energies, where a kinetic preference of the direct bond cleavage would be expected. This points to a very efficient rearrangement of $\mathbf{1}^+$ to isomer $\mathbf{2}^+$ and $\mathbf{3}^+$. As already suggested by the experiment, the consecutive eliminations of two radicals, $CH_3O^•$ and $Cl^•$, can be excluded, because it requires much larger energy than all other channels ($E_{rel}(^4\mathbf{6}^+ + CH_3O^• + Cl^•) = 5.84$ eV), and it is also beyond the collision-energy range explored in the experiments.

In summary, the unimolecular reactivity of the $[(PQ)FeCl(CH_3O)]^+$ complex demonstrates the redox activity of the phenanthraquinone ligand. Without necessity of a spin change at the iron center, which is otherwise typical for the oxidation/reduction processes proceeding at iron,[49] the oxidation of other ligands is allowed.[50] In this manner, two electrons from the oxidation process are transferred to iron and phenanthraquinone, leading to the product complex of iron(II) with phenanthrasemiquinolate. Phenanthraquinone can also act as an acceptor of hydrogen atoms, which leads to the generation of phenanthrasemihydroquinone. We did not find any intermediate, which would suggest a two-electron reduction of phenanthraquinone,[51−53] which means that for such a pathway some other mechanism must be operative.

For comparison, we also report the reactivity of an analogous complex, where 9,10-phenanthraquinone is replaced by 1,10-phenanthroline (phen).[54] The required complex $[(phen)FeCl(CH_3O)]^+$ ($\mathbf{11}^+$) is generated by ESI from the methanolic solution of $FeCl_3$ and phen. The CID spectrum of $[(phen)FeCl(CH_3O)]^+$ shows analogous fragmentations as found for $[(PQ)FeCl(CH_3O)]^+$: losses of HCl, CH_2O, and $CH_3O^•$ and the combined loss of HCl and CH_2O (Figure 1b; Figure S2 in the Supporting Information). The overall fragmentation behavior is, however, distinctively different. While the eliminations of closed-shell molecules prevail for the phenanthraquinone complex, the fragmentation of the phenanthroline complex is dominated by the expulsion of the methoxy radical. The eliminations of closed-shell molecules appear at similar collision energies, but notably the CH_2O elimination is suppressed.

(49) (a) Schröder, D.; Shaik, S.; Schwarz, H. *Acc. Chem. Res.* **2001**, *33*, 139. (b) Shaik, S.; Hirao, H.; Kumar, D. *Acc. Chem. Res.* **2007**, *40*, 532.

(50) Cohn, M. J.; Xie, Ch. L.; Tuchagues, J.-P. M.; Pierpont, C. G.; Hendrickson, D. N. *Inorg. Chem.* **1992**, *31*, 5028.

(51) Taguchi, K.; Fujii, S.; Yamano, S.; Cho, A. K.; Kamisuki, S.; Nakai, Y.; Sugawara, F.; Froines, J. R.; Kumagai, Y. *Free Radical Biol. Med.* **2007**, *43*, 789.

(52) Shimizu, M.; Katsuda, N.; Katsurada, T.; Mitani, M.; Yoshioka, Y. *J. Phys. Chem. B* **2008**, *112*, 15116.

(53) Taguchi, K. *J. Health Sci.* **2009**, *55*, 347.

(54) Brechin, E. K.; Calucci, L.; Englert, U.; Margheriti, L.; Pampaloni, G.; Pinzino, C.; Prescimone, A. *Inorg. Chim. Acta* **2008**, *361*, 2375.

Scheme 5. Optimized Structures of $[(phen)FeCl(CH_3O)]^+$ and Its Isomers[a]

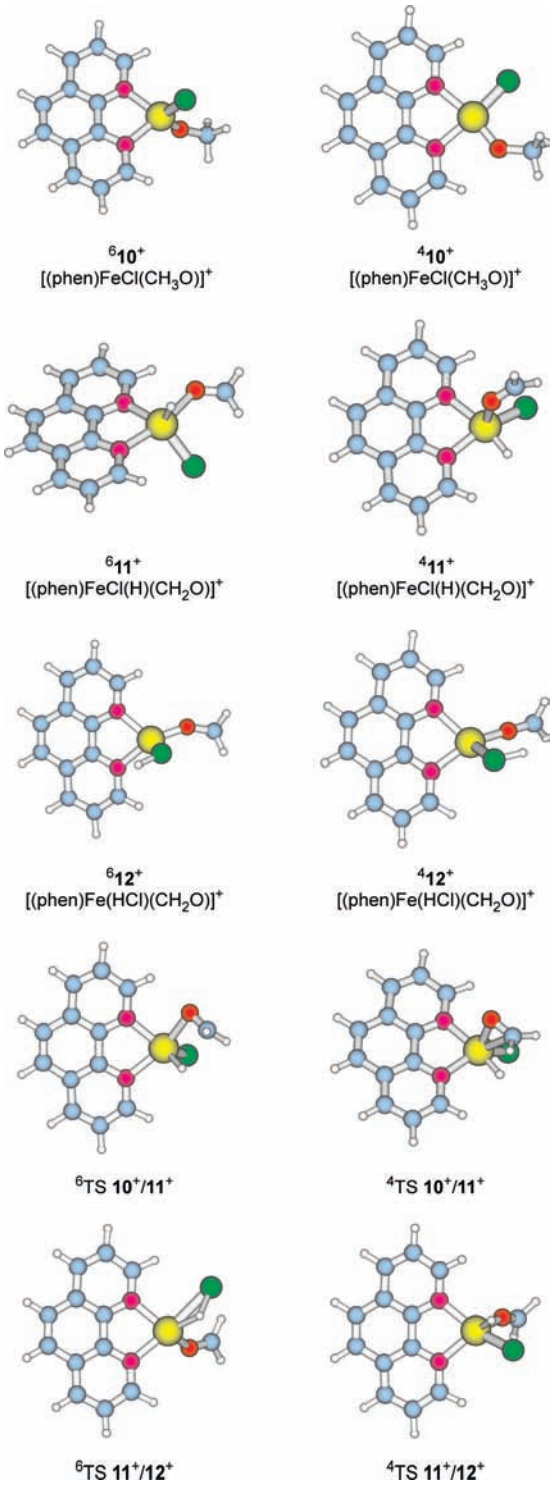

[a] The carbon atoms are in blue, oxygens in red, chlorines in green, nitrogens in purple, hydrogens in white, and iron is yellow. More information can be found in the Suporting Information.

The presence of CH_2O and HCl losses again indicates hydrogen migrations within the complex (Figure 3a, Scheme 5). The calculations provide two alternative isomers with a hydrogen atom bound to either iron or chloride. The initial isomer $[(phen)FeCl(CH_3O)]^+$ has a sextet ground state (^{6}**10**$^+$). The quartet state (^{4}**10**$^+$) lies 0.50 eV higher in energy,

Scheme 6. Optimized Structures of the Elimination Products of the Phenanthroline Complexes[a]

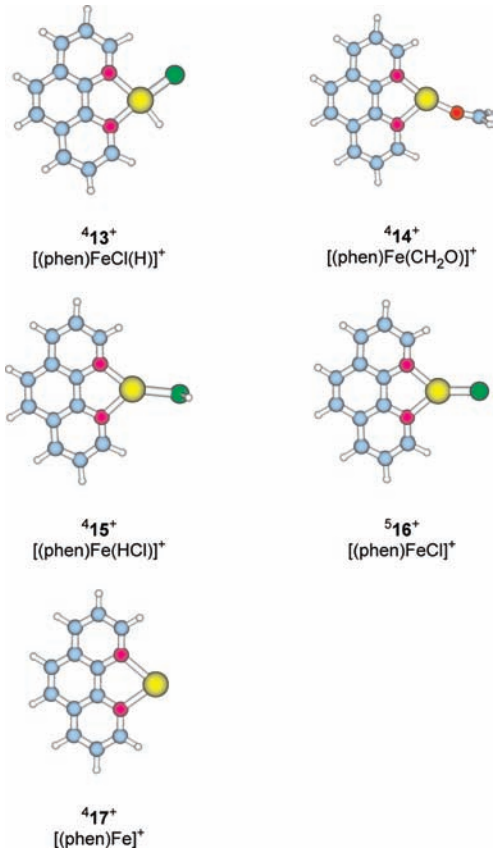

[a] The carbon atoms are in blue, nitrogens in purple, chlorines in green, and hydrogens in white. More information can be found in the Supporting Information.

and the doublet state (^{2}**10**$^+$) is 1.28 eV above the sextet. The ground state of the second isomer with a hydrogen atom bound to iron, $[(phen)FeCl(H)(CH_2O)]^+$ (**11**$^+$), corresponds to a quartet and lies 1.19 eV above ^{6}**10**$^+$. The last isomer bearing HCl and CH_2O ligands, $[(phen)Fe(HCl)(CH_2O)]^+$ (**12**$^+$), also has the quartet ground state and lies 1.39 eV higher in energy than ^{6}**10**$^+$.

The experimental IRMPD spectrum is dominated by a single band at 1088 cm^{-1} (solid line in Figure 3b−d).[55,56] The comparison with the calculated IR spectra of ^{6}**10**$^+$ (Figure 3b), ^{4}**11**$^+$ (Figure 3c), and ^{4}**12**$^+$ (Figure 3d) shows that the experimental band is reproduced only by the spectrum of isomer **10**$^+$ bearing chloride and methanolate counterions. The band at 1088 cm^{-1} corresponds to the CO stretching mode of the methanolate ligand. Hence, the generated complex does not spontaneously undergo rearrangements, and the eliminations of HCl and CH_2O occur only after the collisionally driven rearrangements.

(55) We note that the intensities of peaks in the experimental IRMPD spectra do not directly correlate with the theoretical IR intensities, because usually many photons are necessary to induce the dissociation. See also: Schröder, D.; Schwarz, H.; Milko, P.; Roithová, J. *J. Phys.Chem. A* **2006**, *110*, 8346.

(56) For other examples of low sensitivity of the IRMPD technique towards C−C stretches of aromatic systems, see: (a) Dopfer, O.; Lemaire, J.; Maitre, P.; Chiavarino, B.; Crestoni, M.-E.; Fornarini, S. *Int. J. Mass Spectrom.* **2006**, *149*, 249−250. (b) Lorenz, U. J.; Lemaire, J.; Maitre, P.; Crestoni, M.-E.; Fornarini, S.; Dopfer, O. *Int. J. Mass Spectrom.* **2007**, *267*, 43.

The rearrangement of the initial complex $^6\mathbf{10}^+$ to the intermediate $^4\mathbf{11}^+$ ($E_{rel}(^4TS\mathbf{10}^+/\mathbf{11}^+)$ = 1.65 eV and $E_{rel}(^6TS\mathbf{10}^+/\mathbf{11}^+)$ = 1.95 eV) is associated with a spin crossover and represents, most probably, the rate-determining step on the pathway toward eliminations of closed-shell molecules.[49] The isomer $^4\mathbf{11}^+$ can either directly eliminate the CH_2O molecule or can undergo a further rearrangement toward $^4\mathbf{12}^+$. The energy barrier for the rearrangement ($E_{rel}(^4TS\mathbf{11}^+/\mathbf{12}^+)$ = 1.68 eV) is smaller than the energy demand for the direct CH_2O elimination ($E_{rel}(^4\mathbf{13}^+ + CH_2O)$ = 1.90 eV), which results in a small abundance of this fragmentation channel. The isomer with the HCl and CH_2O ligands, $^4\mathbf{12}^+$, preferentially loses HCl ($E_{rel}(^4\mathbf{14}^+ + HCl)$ = 1.55 eV compared to $E_{rel}(^4\mathbf{15}^+ + CH_2O)$ = 2.37 eV). The combined elimination of both ligands requires 2.97 eV (optimized structures of the elimination products can be found in Scheme 6).

The direct elimination of the methoxy radical from $^6\mathbf{10}^+$ needs 2.08 eV, which is similar to value found for $^6\mathbf{1}^+$. In agreement, the eliminations of $CH_3O^\bullet$ from [(phen)FeCl(CH$_3$O)]$^+$ and [(PQ)FeCl(CH$_3$O)]$^+$ also appear at almost identical energies (Figure 1). This finding shows that this channel is not influenced by the nature of the bidentate ligand bound to iron. The differences between the reactivities within the [(phen)FeCl(CH$_3$O)]$^+$ and [(PQ)FeCl(CH$_3$O)]$^+$ complexes are therefore due to the spin-crossover bottleneck in the first case, which is removed due to the active participation of phenanthraquinone in the redox processes in the second case.

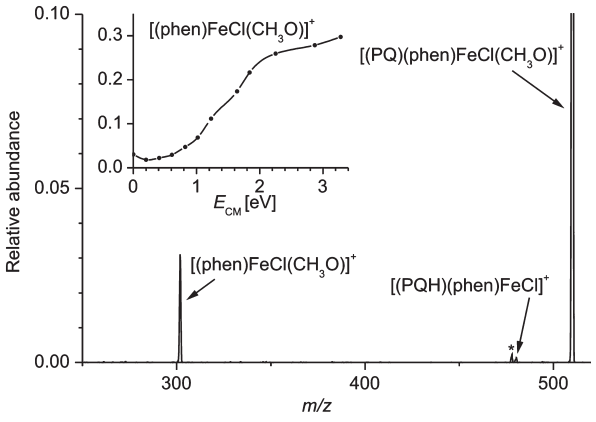

Figure 4. CID spectrum of the mass-selected [(PQ)(phen)FeCl(CH$_2$O)]$^+$ (m/z 510, abundance normalized to 1) at E_{CM} = 0.20 eV. The signal denoted by an asterisk corresponds to the dominant fragmentation of an isobaric impurity (see the Supporting Information). The inset shows the increasing abundance of the PQ loss with the increasing collision energy.

Finally, the effect of phenanthroline on the reactivity of iron(III) with phenanthraquinone in the mixed complex [(PQ)(phen)FeCl(CH$_3$O)]$^+$ is studied. The complex is generated by ESI from a methanolic solution of iron(III) chloride, PQ, and phen. The CID spectrum of [(PQ)(phen)FeCl(CH$_3$O)]$^+$ shows only two fragmentation channels (Figure 4 and S3 in the Supporting Information). The dominant fragmentation corresponds to the loss of PQ. In comparison, no elimination of phen has been detected over the whole interval of collision energies studied. This finding demonstrates that phenanthraquinone is a much weaker ligand for iron(III) than phenanthroline. The minor channel leads to the elimination of formaldehyde with the maximum abundance at nominally zero collision energy, and its abundance continuously decreases with the increasing collision energy.

The computational investigation provides a further insight into the reactivity (Scheme 7). Thus, the electronic structure of the parent compound [(PQ)(phen)FeCl(CH$_3$O)]$^+$ ($\mathbf{18}^+$) corresponds to iron(III) ligated by fully oxidized phenanthraquinone and phenanthroline with two counterions, chloride and methanolate. The ground state corresponds to a sextet, and the excitation energies to the quartet and doublet states amount to 0.34 and 0.46 eV, respectively. The elimination of PQ requires only 0.84 eV. The weaker interaction between PQ and iron in [(PQ)(phen)FeCl(CH$_3$O)]$^+$ ($\mathbf{18}^+$) compared to [(PQ)FeCl(CH$_3$O)]$^+$ ($\mathbf{1}^+$) is also reflected in the geometry of the PQ ligand: The CO bonds are shorter (1.224 Å and 1.234 Å), and the CO stretching vibrations are blue-shifted (1642 cm^{-1}) with respect to those in $\mathbf{1}^+$ (1580 cm^{-1}). In comparison, the elimination of phenanthroline is endothermic by 1.65 eV, and therefore it cannot compete with the PQ elimination in the collision energy range studied.

Scheme 7. Fragmentation Energetics of the [(PQ)(phen)FeCl(CH$_3$O)]$^+$ Complex ($\mathbf{18}^+$)[a]

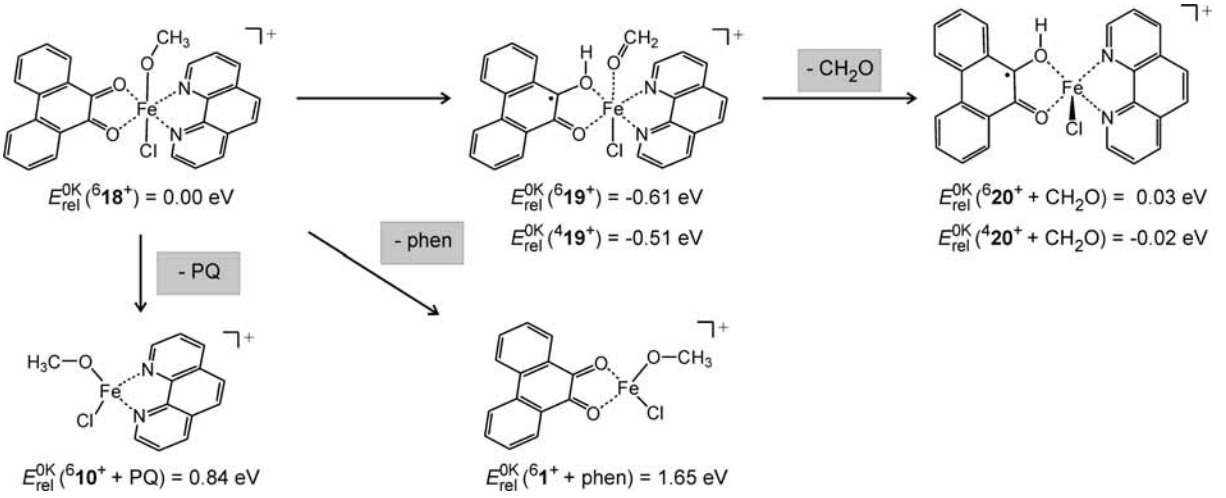

[a] Energies are given at 0 K relative to $E^{0K}(^6\mathbf{18}^+)$ = −3099.333813 hartree. The optimized geometries, energies of excited states, spin densities, and some high-energy isomers can be found in the Supporting Information.

The loss of formaldehyde requires a migration of a hydrogen atom from the methoxy group to iron or one of the ligands. As demonstrated by the missing loss of HCl in the experiment, the migration of a hydrogen atom to chlorine is "switched off" by the geometry of the complex, which bears two bidentate ligands in the plane around iron and the chloride and methanolate counterions in the apexes. In analogy with $\mathbf{1}^+$, we have assumed the migration of a hydrogen atom to phenanthraquinone. The relevant isomer $^6\mathbf{19}^+$ lies 0.61 eV lower in energy than $^6\mathbf{18}^+$, and the subsequent elimination of formaldehyde is almost thermoneutral with respect to the energy of $^6\mathbf{18}^+$ ($E_{rel}(^6\mathbf{20}^+ + CH_2O)$ = 0.03 eV). Both the isomer $^6\mathbf{19}^+$ and the product $^6\mathbf{20}^+$ contain iron(II) and phenanthrasemihydroquinone (the spin-flip at the PQH ligand leads to the quartet states with energies $E_{rel}(^4\mathbf{19}^+) = -0.51$ eV and $E_{rel}(^4\mathbf{20}^+ + CH_2O) = -0.02$ eV).

In summary, the experiment with the complex comprising both studied ligands bound to iron(III) has two important implications. First, the coordination of phenanthroline to the complex of iron(III) facilitates energetically the redox processes occurring between iron and phenanthraquinone. Phenanthroline itself, however, is an "innocent" ligand, as demonstated by the comparative study of $[(phen)FeCl(CH_3O)]^+$. Accordingly, we conclude that the hexacoordination bears the major effect, which facilitates the oxidation of methanolate to formaldehyde concomitant with the reduction of iron(III) to iron(II) and the formation of phenanthrasemihydroquinone. This finding can be crucial for the toxicity of phenanthraquinone, which can produce the harmful semiquinone radicals just in the presence of iron(III) (surrounded by solvent molecules, i.e., always hexacoordinated) and a suitable reductant (e.g., $NADPH^+$) without the necessity of an involvement of any enzyme. Second, the experiment clearly shows that phenanthroline is a much stronger ligand than phenanthraquinone and therefore can replace phenanthraquinone in the iron complexes and block them for further reactivity.

Conclusions

Using a simple gas-phase model $[(PQ)FeCl(CH_3O)]^+$, we have shown that phenanthraquinone takes active part in the redox process occurring at iron and enables the oxidation of methanolate to formaldehyde concomitant with the reduction of iron(III) to iron(II) and the formation of the phenanthrasemihydroquinone radical. The analogous complex $[(phen)FeCl(CH_3O)]^+$ shows typical two-state reactivity, and phenanthroline, an "innocent" ligand, does not actively participate in the redox processes. Finally, the complex containing both investigated ligands, $[(PQ)(phen)FeCl(CH_3O)]^+$, reveals that the hexacoordination of iron energetically facilitates the oxidation of the methanolate counterion. The associated loss of formaldehyde is observed already at zero collision energy, and the calculations suggest that the reaction is thermoneutral. The oxidation is again associated with the formation of the iron(II)/phenanthrasemihydroquinone couple. The experiments also demonstrate that the phen ligand is much stronger bound to iron(III) than PQ, and therefore it can potentially replace PQ in complexes with iron(III) or block the iron complexes for the interaction with PQ.

Acknowledgment. This work was supported by the Grant Agency of the Academy of Sciences of the Czech Republic (KJB400550704) and the Ministry of Education of the Czech Republic (MSM0021620857, RP MSMT 14/63). J.R. and P.M. received a travel grant from the European Commission to the European multiuser facility CLIO. The authors thank J. Lemaire for his help during the measurements at CLIO and P. Sládek for help with programming a CLIO data analysis program.

Supporting Information Available: CID spectra, IRMPD spectra, broken-symmetry calculations, optimized geometries, and total energies are available free of charge via the Internet at http://pubs.acs.org.